



Simulation of the retardation effect after applying a simple overload on alloys of aluminum 2024T351 using the Willemborg model

Kaddour Bahram

University Centre of Ain Témouchent-Belhadj Bouchaib, Department of Mechanical Engineering, Po Box 284,46000, Algeria
Laboratory of Materials and Reactive Systems LMSR, Department of Mechanical Engineering, University Djilali Liabes, BP 89, Cité Ben M'hidi, Sidi bel Abbès, 22000, Algeria
Kadero_7@hotmail.com, <https://orcid.org/0000-0002-8963-4936>

Mohamed Chaib

Smart Structures Laboratory (SSL) University Centre of Ain Témouchent-Belhadj Bouchaib, Po Box 284,46000, Algeria.
pro19mob@hotmail.com, <https://orcid.org/0000-0002-0493-1764>

Abdelkader Slimane, Benattou Bouchouicha

Laboratory of Materials and Reactive Systems LMSR, Department of Mechanical Engineering, University Djilali Liabes, BP 89, Cité Ben M'hidi, Sidi bel Abbès, 22000, Algeria
slimane.aek@hotmail.com, <https://orcid.org/0000-0001-5183-7420>
benattou_b@yahoo.fr, <https://orcid.org/0000-0002-6051-5108>



ABSTRACT. The structures in service are subjected to loads whose amplitude varies most often over time. These differences in loading cycle levels will have a direct impact on the propagation of cracks that can lead to accelerations or slowdowns in the propagation speed of these cracks.

Indeed, the delay of the propagation of a crack produced by the application of a simple overload depends on several parameters, such as the material, the loading, the geometry of the specimen and the environment.

In this paper, study the influence of the loading parameters such as the load ratio, and the overload rate, on both crack propagation, propagation speed, number of delay cycle, is investigated by using the AFGROW code and the willenbourg model, which describes the delay after applying overloads.

KEYWORDS. Aluminum alloys; 2024T351; Fatigue; Plastic zone; Simple overload; Willenbourg model.

Citation: Bahram, K., Chaib, M., Slimane, A., Bouchouicha, B., Simulation of the retardation effect after applying a simple overload on alloys of aluminum 2024T351 using the Willemborg model, *Frattura ed Integrità Strutturale*, 51 (2020) 467-476.

Received: 28.09.2019

Accepted: 11.12.2019

Published: 01.01.2020

Copyright: © 2020 This is an open access article under the terms of the CC-BY 4.0, which permits unrestricted use, distribution, and reproduction in any medium, provided the original author and source are credited.

INTRODUCTION

The prevention of breaks in service is an ongoing objective of designers, builders and users, in both energy sector (thermal power stations, alternators), oil sector (gas pipelines, pipelines), aeronautical sector (cells), rail and road transport, public works (bridges, dams, piers), consumer goods (automobiles) [1-3].



Structures subjected to cyclic loadings can undergo large variations in their behaviour ranging from the phase of plastic deformation to breaking through damage depending on the nature of the stresses. The constant nature of these stresses at constant amplitude implies the use of laws and models which are mastered by the current computation codes, currently, the PARIS law is the expression most used in fatigue research work with constant amplitude, it should be noted that this relation is applicable only in the field of slow crack propagation (domain II) and it does not take into account what happens in domain I and III [4-6].

Nevertheless, the constant amplitude propagation laws make it possible to describe the propagation of long cracks under constant amplitude loading. Indeed, it is implicitly assumed that a given cycle causes a loss assimilated to an advance regardless of the history of previous loading. However, actually, the structures are only very rarely subjected to loads of constant amplitude. On the other hand, the load spectrum measurements indicate a variation of the stress amplitude over time. In addition, experience shows that the damage induced by a given cycle may depend on the previous history of loading [7-9].

It has now been found that the application of an overload cycle during a fatigue crack propagation leads to a slowing of the crack propagation speed, in some cases to a stop of this crack [10-12], this phenomenon of delay due to the application of an overload, several authors [13-15], proposed different models to explain the causes due to the slowing of the crack propagation speed. These different approaches can be grouped into three categories of models, based on:

- i) the interaction effects of the plastic areas at the tip of the crack. These models are inspired by that of Wheeler [14].
- ii) the phenomenon of closing the crack due to the residual stresses induced by the plastification near the crack tip. These models are based on that of Elber [13].
- iii) micromechanisms that act at the tip of the crack. These models are inspired by [16-18], in the case of an elastoplastic material. The strongly deformed area near the crack. is governed by an oligocyclic fatigue mechanism.

In the following, we will use the AFGROW calculation code and the model describing the delay of Willembourg to study the influence of the application of simple overload on different parameters such as, crack spread, crack rate and overload rate.

WILLENBORG MODEL

The Willenborg model is a slightly different approach since it proposes to determine a slowing factor [15], but an actual value of the ratio of load at crack point R_{eff} .

The formulation of the generalized Willenborg model implemented in the AFGROW code is shown below:

$$R_{eff} = \frac{K_{min\,eff}}{K_{max\,eff}} \quad (1)$$

with

$$K_{min\,eff} = K_{min} - K_R \quad (2)$$

$$K_{max\,eff} = K_{max} - K_R \quad (3)$$

The value of the residual stress intensity factor K_R is defined for a crack length a_i , necessary to create a plasticized zone of size R_{eq} , tangent the plasticized zone created by the overload R_{pic} .

$$\begin{cases} \text{if } K_{min\,eff} > 0 \text{ and } K_{max\,eff} > 0, \Delta K_{eff} = \Delta K \\ \text{if } K_{min\,eff} < 0 \text{ and } K_{max\,eff} < 0, \Delta K_{eff} = \Delta K_{max\,eff} \\ \text{if } K_{max\,eff} < 0, \Delta K_{eff} = 0 \end{cases} \quad (4)$$

The residual stress intensity factor is given by the following equation:



$$K_R = \phi \left(K_{pic} \sqrt{1 - \frac{a_i - a_0}{R_{pic}}} - K_{max} \right) \quad (5)$$

where R_{eq} is expressed by the following equation:

$$R_{eq} = \left(\frac{K_{max} + K_R}{\sigma_y} \right)^2 \left(\frac{1}{\alpha\pi} \right) \quad (6)$$

α is state of stress in the direction of propagation of the crack (plane stress or plane strain), and ϕ define the level of residual stress induced by application of overload, it is given by the following equation:

$$\phi = \frac{\left(1 - \frac{\Delta K_{THO}}{\Delta K} \right)}{SOR - 1} \quad (7)$$

where

ΔK_{THO} represents the threshold stress intensity factor for a load ratio $R = 0$.

SOR: Shut-off Ratio - Ratio of overload maximum stress to the subsequent maximum stress required to arrest crack growth. The value of K_{pic} is updated whenever the maximum load exceeds the previous maximum value, or when the current plasticized area extends beyond the area created by the overload.

The exact value of the SOR is varied to adjust the life prediction to match test results. Ideally, the SOR should be a material parameter that is insensitive to spectrum or stress level. However, this does not always work out. The following is a list of common SOR values for some materials:

As an indication, $SOR = 2$ for the steels, $SOR = 2.7$ for the titanium alloys and $SOR = 3$ for the aluminum alloys.

It is therefore assumed that the delay disappears as soon as the current plasticized zone enters a zone of material not affected by the overload.

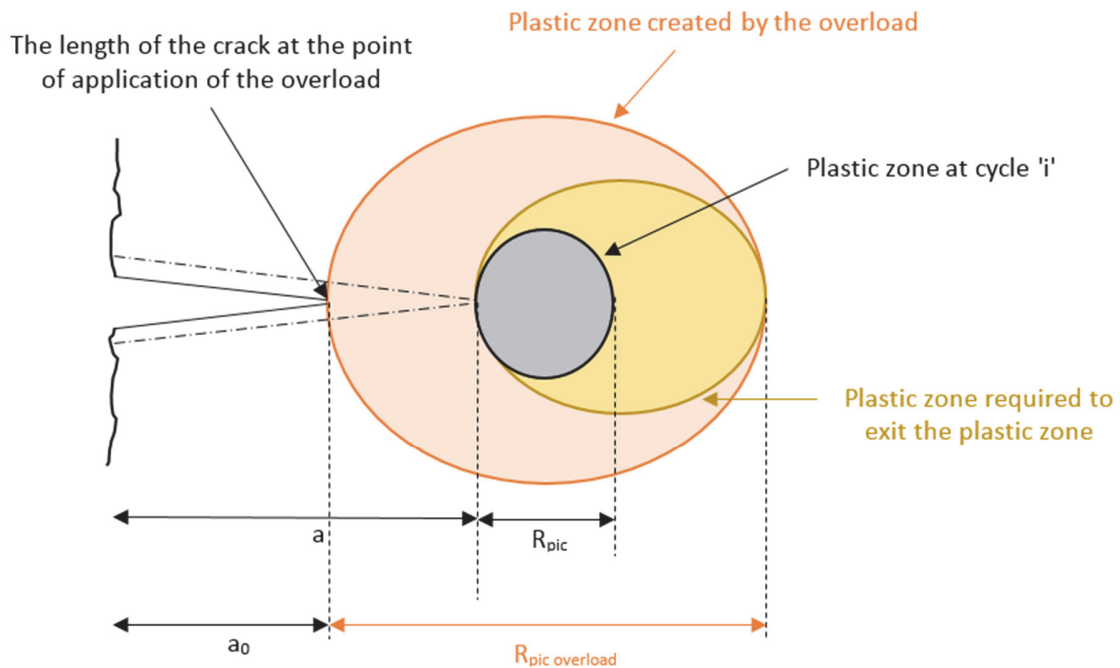


Figure 1: Willenborg retardation model



FATIGUE CRACK GROWTH MODEL

The NASGRO model used in the prediction of the fatigue crack growth rate was developed by Forman [19] to take into account the entire propagation curve.

The NASGRO equation is shown below:

$$\frac{da}{dN} = C \left[\left(\frac{1-f}{1-R} \right) \Delta K \right]^n \frac{\left(1 - \frac{\Delta K_{th0}}{\Delta K} \right)^p}{\left(1 - \frac{K_{max}}{K_{crit}} \right)^q} \tag{8}$$

where:

ΔK is the stress intensity range.

ΔK_{max} is the maximum stress intensity range

ΔK_{TH0} is the threshold stress intensity range at the stress ratio R under consideration.

K_{crit} critical stress intensity factor

f is the Newman crack closure function [20].

The parameters C, n, p, are determined experimentally, where:

C : is a constant for the case where stress ratio R=0

n : is the slope on a log-log scale

p and q are empirical coefficients that determine the curvature of the growth rate curve in the tail regions. Their values are selected to fit the growth rate curve to experimental data. The coefficient p controls the curve in the low growth rate (threshold) region, and q controls the curve in the high growth rate region.

CASE STUDY

This study was conducted on aluminum alloys 2024 T351, whose mechanical properties are increased by a heat treatment to adulterate its micro-structure. This material is widely used in aeronautics and automobile industry.

The mechanical properties as well as the NASGROW parameters used in the simulation are given in Tab. 1 and 2 .

E (MPa)	σ_e (MPa)	σ_{max} (MPa)	ϵ rupture (%)
74000	365	415	12.8

Table 1: Mechanical properties of the aluminum alloy 2024 T351 (AFGROW database).

Aluminum alloy	ΔK_{th0} MPa√m	K_{IC} MPa√m	K_C MPa√m	n	p	q	c
2024T351	2.857	37.36	74.72	3	0.5	1	1.707*10 ⁻¹⁰

Table 2: Propagation model parameters useful by the NASGRO model (AFGROW database).

For the simulations, we used a CT 50 specimen (Fig. 2); the specimen is subjected to a mode I loading.

We chose to study the propagation of cracks under mode I because it is considered the most dangerous due to the opening by traction, which favors the initiation and the propagation of the cracks.

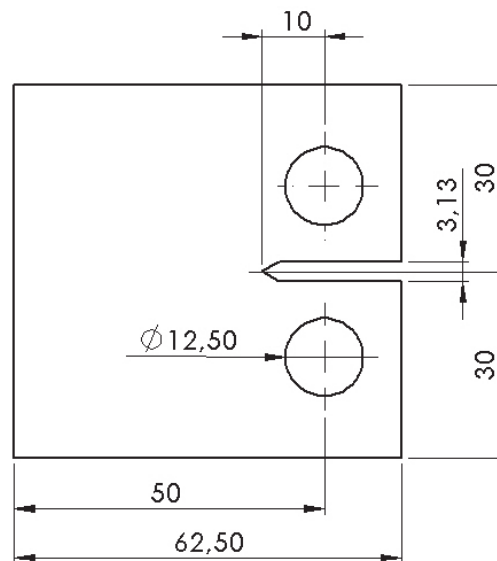


Figure 2: Detail of the CT50 specimen.

INFLUENCE OF THE OVERLOAD ON THE CRACK PROPAGATION

For the rest of the simulations, and in order to observe the influence of the overloads on the crack propagation, we proceed to the application of the overloads (Tab. 3) for the different load ratios 0.1, 0.5, and 0.7.

Load ratio	P_{\max} (KN)	P_{\min} (KN)	Number of loading cycles
0.1	4	0.4	40 000
	10	0.4	1
	4	0.4	200000
0.5	4	2	150 000
	10	2	1
	4	2	500 000
0.7	4	2.8	500 000
	10	2.8	1
	4	2.8	1 600 000

Table 3: Loading Parameters.

Fig. 3 shows that for different load ratios 0.1, 0.5 and 0.7, after the application of the overload, the delay phenome is observed.

We also observe for the three load ratios, only after the application of the overload the slope of the crack propagation curve decreased during a number of delay cycles (N_d), this change of slope is affected by the creation of a plastic zone around the crack and once the crack passes through this area, it recovers its initial slope.

It is also noted that the number of delay cycles is different from one load ratio to another, this is certainly due to the difference of the overload rate between 0.1, 0.5 and 0.7.

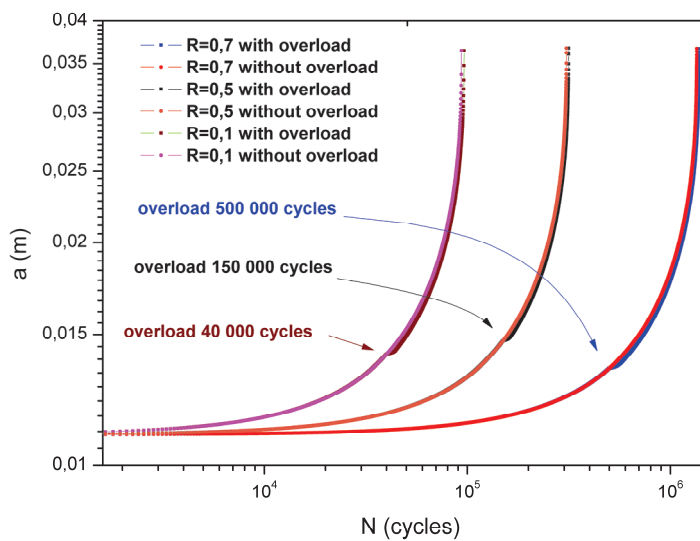


Figure 3: Crack propagation evolution before and after application of the overload for the different load ratios.

INFLUENCE OF OVERLOADS ON THE CRACKING RATE

Figure 4 illustrates the evolution of the cracking rate as a function of the number of loading cycles. By analysing this figure, several observations can be made between them.

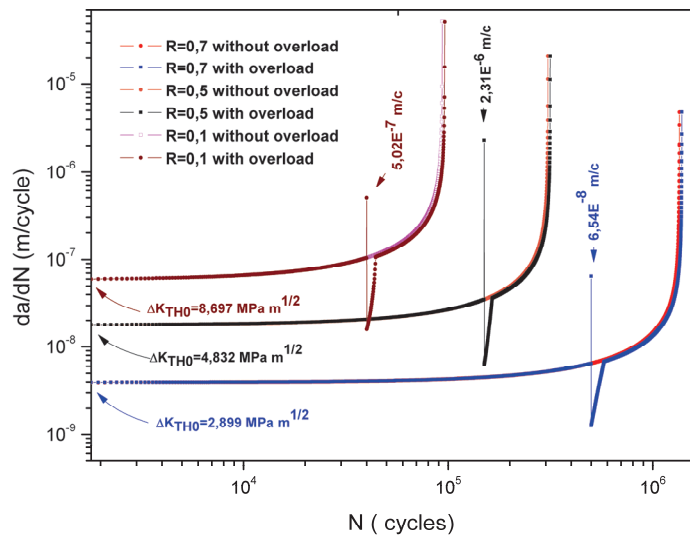


Figure 4: Evolution of the cracking rate as a function of the number of loading cycles.

- (i) It is noted that for different load ratios, after application of the overload the cracking rate is affected by the application of the overload.
- (ii) The cracking speed after applying the overload goes mainly through four steps:
 - 1- First stage: an increase in the cracking rate with a slight slope is observed.
 - 2- Second stage: by applying the overload, the cracking rate increases very rapidly for recorded in pic.
 - 3- Third stage: a rapid drop in the cracking rate may be observed to reach a minimum value noted (da / dN_{min}) . This area strongly disturbed by the overload corresponds to a crack length a_{min} .
 - 4- Fourth stage: the cracking rate begins to increase gradually in the plasticized zone created by the application of the overload, until it returns to almost its initial value (da / dN) before application of the overload.



We also notice, for the three load ratios the maximum cracking rate (da / dN_{max}) recorded after the application of the overload is different from one load rate to another, this difference certainly has a major impact on the size of the plastic zone created by the application of the overload and consequently on the number of delay cycles.

INFLUENCE OF THE OVERLOAD RATE

In order to better understand the influence of the overload rate on the various parameters, only one load ratio ($R = 0.5$) is considered in the following (Tab. 4).

Overload rate	P_{max} (KN)	P_{min} (KN)	Number of loading cycles
2.5	4	2	150 000
	10	2	1
	4	2	500 000
2	4	2	150 000
	8	2	1
	4	2	500 000

Table 4: Loading parameters.

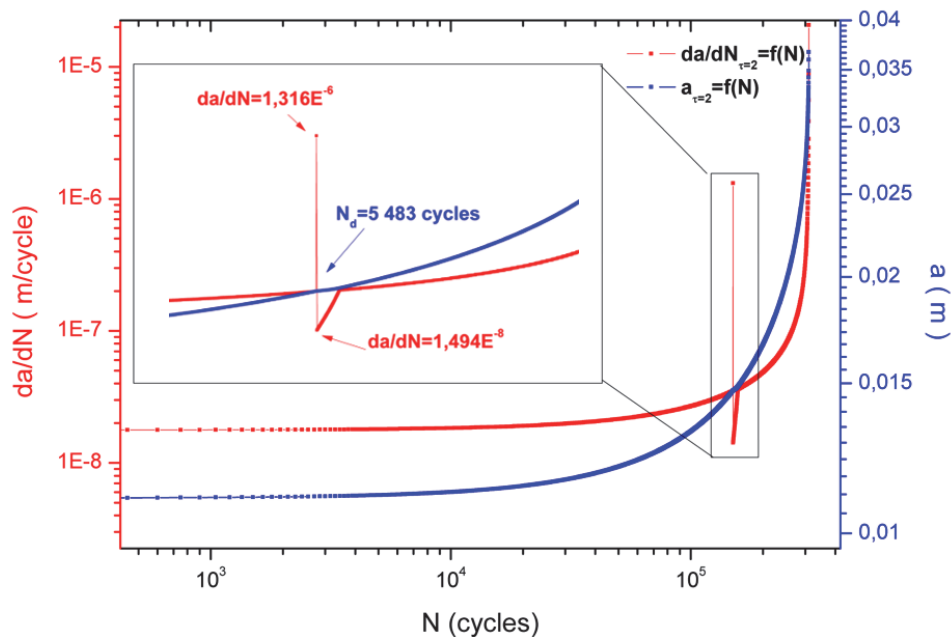


Figure 5: Evolution of the cracking rate and crack propagation as a function of the number of cycles for an overload rate ($\tau = 2$).

By observing both Figs. 5 and 6, we can deduce and advance several conclusions:

- 1- The overload rate has a direct influence on several parameters such as the cracking speed, the propagation of the crack as well as da / dN_{max} and da / dN_{min} after applying the overload.
- 2- It can also be concluded that an increase in the overload ratio systematically increases the two peak cracking rate either da / dN_{max} and da / dN_{min} , which also increases the number of delay cycle.
- 3- We notice a decrease in the slope of the crack propagation curve, this regression is due to the formation of the plastic zone in the vicinity of the crack, the crack will not leave this zone until after a certain number of delay cycles . this regression is due to the formation of the plastic zone in the vicinity of the crack, the crack will not leave this

zone until after a certain number of delay cycles., that is equal to 5438 cycles for the overload rate equal to 2 and 20,727 cycles for an overload rate of 2.5.

- 4- The difference in the numbers of cycles delay is due to the size of the plastic zone, the one created by the overload rate equal to 2.5 is greater than that created by the overload rate equal to 2, which explains why the crack takes more cycles to get out of this zone to reach the same cracking rate before the application of the overload.

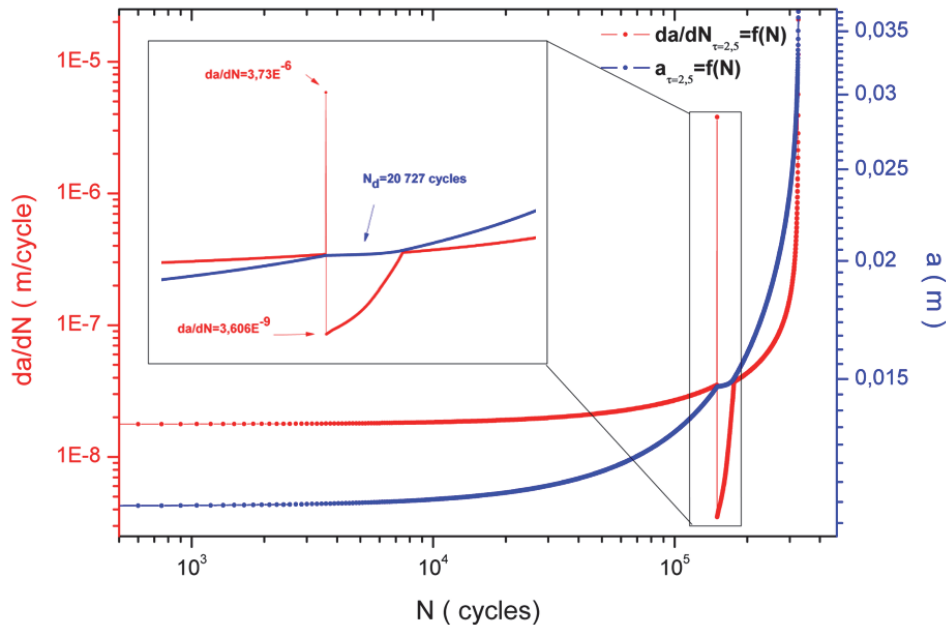


Figure 6: Evolution of the cracking rate and crack propagation as a function of the number of cycles for an overload rate ($\tau = 2.5$).

CONCLUSION AND PERSPECTIVES

Following this study, which was conducted to predict the fatigue behavior of aluminium 2024T351 used in aircraft construction, and in light of the results presented, it can be concluded that:

The application of a simple overload affects several parameters, such as the cracking rate, crack propagation and the number of delay cycles.

Whatever the load ratio 0.1, 0.5 or 0.7, after applying the overload, the cracking rate increases until it reaches a maximum value da / dn_{max} , then it decreases until it reaches a minimum value da / dn_{min} , then it begins to increase gradually until it reaches its initial value before application of the overload.

The overload rate has a major impact on the number of delay cycles, increasing the overload rate increases the number of delay cycles.

The overload rate is also the parameter responsible for the size of the plastic zone, increasing this parameter increases the size of the plastic zone which greatly increases the number of delay cycles

This modest work has allowed us to better understand the influence of overloads on the propagation of fatigue cracks, for future work may be considered such as:

- Study the influence of the application of blocks of overloads, or underloads or both handsets together.
- proceeded to a comparative study between different models which describe the delay.
- study repair structures by patch under a variable load

REFERENCES

- [1] Ricardo, L. C. H and Miranda, C. A. J, (2016). Crack simulation models in variable amplitude loading-a review, *Frattura ed Integrità Strutturale*, 10(35), pp. 456-471, DOI: 10.3221/IGF-ESIS.35.52.



- [2] Benachour, M., Benguediab, M., and Benachour, N. (2013). Notch fatigue crack initiation and propagation life under constant amplitude loading through residual stress field, in *Advanced Materials Research*, 682(2013), pp. 17-24. DOI: 10.4028/www.scientific.net/AMR.682.17.
- [3] Mahmoud, S. and Lease, K. (2004). Two-dimensional and three-dimensional finite element analysis of critical crack-tip-opening angle in 2024-T351 aluminum alloy at four thicknesses, *Engineering fracture mechanics*, 71(9), pp. 1379-1391. DOI: 10.1016/S0013-7944(03)00167-X.
- [4] Papisidero, J., Doquet, V., and Mohr, D. (2015). Ductile fracture of aluminum 2024-T351 under proportional and non-proportional multi-axial loading: Bao–Wierzbicki results revisited, *International Journal of Solids and Structures*, 69(70), pp. 459-474, DOI: 10.1016/j.ijsolstr.2015.05.006.
- [5] Fitzka, M. and Mayer, H. (2016). Constant and variable amplitude fatigue testing of aluminum alloy 2024-T351 with ultrasonic and servo-hydraulic equipment, *International Journal of Fatigue*, 91(2), pp. 363-372, DOI: 10.1016/j.ijfatigue.2015.08.017.
- [6] Henkel, S., Liebelt, E., Biermann, H. and Ackermann, S., (2015). Crack growth behavior of aluminum alloy 6061 T651 under uniaxial and biaxial planar testing condition, *Frattura ed Integrità Strutturale*, 9(34), DOI: 10.3221/IGF-ESIS.34.52.
- [7] Moreno, B., Martin, A., Lopez-Crespo, P., Zapatero, J., and Dominguez, J., (2016). Estimations of fatigue life and variability under random loading in aluminum Al-2024T351 using strip yield models from NASGRO, *International Journal of Fatigue*, 91(2), pp. 414-422, DOI: 10.1016/j.ijfatigue.2015.09.031.
- [8] Wang, D.Q., Zhu, M.L. and Xuan, F.Z. (2017). Crack tip strain evolution and crack closure during overload of a growing fatigue crack, *Frattura ed Integrità Strutturale*, 11(41), pp. 143-148, DOI: 10.3221/IGF-ESIS.41.20.
- [9] Gates, N.R., Fatemi, A., Iyyer, N. and Phan, N. (2016). Fatigue crack growth behavior under multiaxial variable amplitude loading, *Frattura ed Integrità Strutturale*, 10(37), pp. 166-172, DOI: 10.3221/IGF-ESIS.37.23.
- [10] Rodopoulos, C.A. and Kermanidis, A.T. (2007). Understanding the effect of block overloading on the fatigue behaviour of 2024-T351 aluminium alloy using the fatigue damage map, *International journal of fatigue*, 29(2), pp. 276-288, DOI: 10.1016/j.ijfatigue.2006.03.008.
- [11] Maligno, A.R., Citarella, R., and Silberschmidt, V.V. (2017). Retardation effects due to overloads in aluminium-alloy aeronautical components, *Fatigue & Fracture of Engineering Materials & Structures*, 40(9), pp. 1484-1500, DOI: 10.1111/ffe.12591.
- [12] Zhang, L., Gao, Q., Ma, S. and Tong, D. (2018). Analysis of Crack Growth Retardation after Single Overload Based on FEM Simulation and CORPUS Model Prediction, in *IOP Conference Series: Materials Science and Engineering*. 28–29 December 2017, Shanghai, China.
- [13] Elber, W. (1971). The significance of fatigue crack closure, in *Damage tolerance in aircraft structures*, ed: ASTM International, pp.230-242. DOI: 10.1520/STP26680S.
- [14] Wheeler, O.E. (1972). Spectrum loading and crack growth, *Journal of basic engineering*, 94(1), pp. 181-186, DOI: 10.1115/1.3425362.
- [15] Willenborg, J., Engle, R. and Wood, H. (1971). A crack growth retardation model using an effective stress concept, *Air Force Flight Dynamics Lab Wright-Patterson*. DOI: 10.0000/apps.dtic.mil/ADA956517.
- [16] Hutchinson, J. (1968) Singular behaviour at the end of a tensile crack in a hardening material, *Journal of the Mechanics and Physics of Solids*, 16(1), pp. 13-31, DOI: 10.1016/0022-5096(68)90014-8.
- [17] Rice, J., (1967) Mechanics of crack tip deformation and extension by fatigue, in *Fatigue crack propagation*, ed: ASTM International, pp.247-311, DOI: 10.1520/STP47234S.
- [18] Rice, J. and Rosengren, G.F., (1968) Plane strain deformation near a crack tip in a power-law hardening material, *Journal of the Mechanics and Physics of Solids*, 16(1), pp. 1-12, DOI: 10.1016/0022-5096(68)90013-6.
- [19] Forman, R.G. and Mettu, S.R. (1990). Behavior of surface and corner cracks subjected to tensile and bending loads in Ti-6Al-4V alloy, *NASA Technical Memorandum ID:19910009960*.
- [20] Newman, J.J. (1984) A crack opening stress equation for fatigue crack growth, *International Journal of fracture*, 24(4), pp. 131-135, DOI: 10.1007/BF00020751.

NOMENCLATURE

R	: Stress ratio.
R_{eff}	: Effective load ratio.



$K_{\min\text{eff}}$: Effective minimum stress intensity factor.
K_{\min}	: Minimal values of the stress intensity factor during a cycle.
K_{\max}	: Maximum values of the stress intensity factor during a cycle.
a_0	: Crack length.
a_0	: Initial crack length.
a_i	: crack length.
C, n	: Material constants of fatigue crack growth.
da / dN	: Fatigue crack growth rate.
da / dN_{\max}	: Maximum speed da / dN after applying the overload.
da / dN_{\min}	: Minimum speed da / dN after applying the overload.
α	: Describes the state of constraint.
K_{pic}	: Maximum value of stress intensity factor at the application of overload.
K_{crit}	: critical stress intensity factor.
R_{pic}	: Maximum value of load ratio at the application of overload.
R_{eq}	: Size of the equivalent plastic zone
ΔK_{eff}	: Effective stress intensity factor range
ΔK	: Stress intensity factor range
K_R	: Residual stress intensity factor due to overload
ϕ	: The level of residual stress induced by application of overload
ΔK_{TH0}	: The threshold stress intensity factor for a load ratio $R = 0$
$SOR = \tau_{crit}$: Critical value of the overload rate resulting in a stop of the propagation of the crack.
P_{\max}	: Maximum load
P_{\min}	: Minimum load
E	: Young's modulus
ε	: Deformation.
τ	: overload rate.